Development of a Model for the Estimation of the Energy Consumption Associated with the Transportation of CO$_2$ in Pipelines

Steven Jackson [ID]

UiT—The Arctic University of Norway, 9019 Tromsø, Norway; steve.jackson@uit.no

check for updates

Abstract: All Carbon Capture and Storage (CCS) projects require the transportation of CO$_2$ from a source to a storage location. Although, a compressor and a large diameter pipeline is the normal method used to achieve this, liquefaction, shipping and pumping is sometimes attractive. Identifying the economic optimum is important for all CCS projects, minimizing energy consumption is also important because it corresponds to a resource efficiency in fossil-fuel based projects. This article describes the development and validation of a model that estimates the energy consumption associate with CO$_2$ transportation using the geographic location of the source and the reservoir to incorporate ambient temperature and bathymetry data. The results of the validation work show an average absolute temperature and pressure error less than 1 °C and 1 bar compared to a reference model. The model has been developed using openly accessible data and is made available in a repository for open research data.

1. Introduction

There are currently 19 large-scale Carbon Capture and Storage (CCS) projects in operation worldwide [1], but to achieve the level of CO$_2$ emissions in the International Energy Agency's Sustainable Development Goals (SDGs) the number of industrial scale facilities will need to increase to more than 2000 by 2040 [2]. Each of these projects requires the transportation of CO$_2$ from a point of origin to a storage location and, since the transportation distance is often significant, over 200,000 km of CO$_2$ pipelines will be required by 2050 by CCS projects [3]. Although the majority of CO$_2$ is likely to be transported using pipelines, the success of many future CCS projects will depend on transportation using ships. For example, the Northern Lights Project, which will be one of the first full-chain projects in Europe [4], is based on ship transportation of CO$_2$ from a source to a hub where a sub-sea pipeline will then connect to the storage location in the Norwegian Sea.

Research supporting the design of CO$_2$ transportation processes has been widely published. A particular focus has been CO$_2$ mixture properties in high-pressure pipelines [5–9], but many other aspects of CO$_2$ pipeline design have been studied, including heat transfer [10–12], transient flow behavior [13] and economic optimization [14–16], to name some examples. Although less research has focused specifically on ship-based transportation, there are still a large number of studies looking at both technical and economic aspects of CO$_2$ shipping [17–19], and a particular focus being the energy consumption associated with the compression and liquefaction processes [20–25].

Figure 1 presents an illustration of the CCS value chain. The illustration indicates that the break-point between the capture and transportation is not always clear-cut, reflecting the fact that some capture processes produce CO$_2$ at elevated pressure. Based on this, and because the capture process is normally the main contribution to overall energy consumption, the full chain, rather than transportation

in isolation, is often the focus of research work. However, the transport energy consumption and the capture unit energy consumption are often independent: One capture option can having multiple possible transportation possibilities with differing energy consumption.
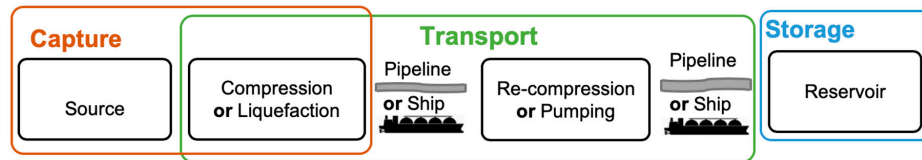
Figure 1. Simplified Illustration of a Typical CCS Value Chain.

In the context of the economic basis for specific CCS projects the selection of the optimum transportation alternative is normally studied. For example, Jakobsen, et al. studies the transportation alternatives associated with the Norcem Brevik cement plant CCS project [26]. Also, to support the economic assessment of CCS projects in general, tools for modelling full CCS chains have been developed that allow comparison of different transportation cases, for example Jakobsen, et al. [27]. Studies have also been conducted in the identification of a more general economic trade-off distance between shipping and pipelines, for example Mallon, et al. [28].

The purpose of the model presented here, in contrast to other work, is to allow the study and comparison of different CO_2 transportation chains on the basis of their energy consumption. The purpose of this article is to present details of how the model was developed and tested.

The model presented here is currently limited to pre- and post-combustion CO_2 stream composition and transportation scenarios in the North, Norwegian and Barents Seas. The inclusion of performance data for different CO_2 sources is planned for future development. The intended use of the model is not as a replacement or competitor to other modelling approaches, but as a tool that enable a perspective on CCS project alternatives focused on energy consumption. Case studies and sensitivity analysis using the mode will be developed and presented as part of future work.

2. Methods

The model described here was developed in Matlab [29] to take advantage of several useful built-in functions, particularly those available via the Mapping and Curve Fitting toolboxes, both of which are required to allow the model to run. The model is built-up from a set of 'functions' that can be called using a 'script' called *Main*. In the following description all of the files that make up the model are referred to using *italics* to highlight their significance. All of the data required for the model to run is incorporated into the model. A summary of the functions that make-up the model and the basis data which is used is provided in Table 1.

Table 1. Summary of Functions and Basis Data.

Functions	Description	Basis Data	Description
CO2TransModel	Main function taking input data from *Case*, passes data to other functions and formats the results.	*Case*	The description of the CCS transport scenario considered. User input.
PipeProf	Calculated the elevation profile based on *Case*.	*Bath* *SSTdata*	Bathymetry basis data Sea temperature basis data
PressProf *PressureDrop* *fFact* *Visc*	Calculates pressure and temperature profiles based on *PipeProf* & stream properties data. Pressure drop used in *PressProf*. Friction factor used in *PressureDrop*. Viscosity calculation.	*Post* *Pre* *Oxy* *	Stream properties data including: compositions, density data, critical constants, dew-point, bubble-point, JT coefficient, heat capacity.
TransEnergy	Calculates energy consumption for compression OR liquefaction and pumping based on *PressProf* and the *SSTdata*.	*CompPost* *CompPre* *CompOxy* * *Liq_Power*	Data relating to the energy consumption for compression, liquefaction and pumping of CO_2 at different pressure and temperature conditions.

* Data available in the model, but not implemented in the *TransEnergy* calculations.

A description of each the model input, calculation methods, basis data and outputs is presented below under several headings.

2.1. Case Defenition

An interface to the model is provided in the script *Main*, which contains guidance on defining the basis for running the model. The basis for any particular case is stored as variables in a 'structure' called *Case*. A summary of the required input data for *Case* is provided in Table 2.

Table 2. Summary of Model Input Parameters.

Name	Description
POI	Geographic reference points (decimal degrees) describing the pipeline route **
Opt	Transport type: 1 = pipeline *; 2 = ship
LiqLoc	Location of the liquefaction process (*Opt* = 2 only) in decimal degrees
WH_loc	Wellhead location: 0 = sub-sea * and 1 = surface wellheads
Res_Depth	Reservoir depth in meters **
Pipe_e	Roughness in µm, default is 15 µm
Stream	'Post' *, 'Pre' or 'Oxy' composition
T_inlet	Pipeline inlet temperature
U	Heat transfer coefficient, default value is 6 W/m^2-K
Flow	Case flowrate in Mtpa **
T_sea	Sea water temperature in °C ***
Pipe_prof	Elevation profile ***

* Default option in the model ** Default is Melkøya based on *** Optional user input: replaces default methods.

CO_2 originating from different emission sources will often have different composition. This impacts on the phase behavior of the mixture and pipeline operating conditions. To take account of this in the model and to maintain consistency with earlier work, three CO_2 mixtures can be selected in the model by specifying either 'Post', 'Pre' or 'Oxy' as the *Stream* in *Case*. These stream alternatives represent a post-combustion capture process from flue gas using a chemical solvent, a pre-combustion capture process from syngas (also using physical solvent) and an oxyfuel flue gas originating from an oxyfuel purification unit. Table 3 summarizes the composition of these streams.

Table 3. CO_2 Mixture Compositions.

Component	Post	Pre	Oxyfuel
CO_2 mole %	99.99	99.50	96.16
N_2 mole %	0.01	-	2.45
CH_4 mole %	-	0.50	-
Ar mole %	-	-	0.96
O_2 mole %	-	-	0.43

Several example cases are made available for use with the model and can be called using *Main*. Alternatively, the user can simply create their own *Case* structure using the parameters from Table 2, or they can simply run *Main* without alteration, which returns results with the default parameters specified in *Case*.

Within *Main* plotting and saving behavior can also be specified using a parameter called *Plot*, which defines the level of plot data generated: 0 = no plots, 1 = simple plots and 2 = all plots, and a parameter called *Save*, which can be set to either 1 = save results, or 0 = no save. Running *Main* calls the function *CO2TransModel*, which subsequently calls the other functions listed in Table 1.

2.2. Pipeline Elevation Profile and Sea Temperature

Pressure changes in CO_2 pipelines occur due to frictional loss, elevation change and acceleration. As the latter is very small compared to the others it is excluded from the present model. Both of the

other effects must be adequately accounted for to ensure an accurate model. Frictional pressure loss varies with pipeline length while changes in static pressure depend on pipeline elevation. Length and elevation data is used by the model in the form of the pipeline profile called *Pipe_prof*, which is generated using the *PipeProf* function and basis data from *Case*. Within *PipeProf* the profile is calculated using the *POI* defined in Case and the basis data defined in *Bath*.

The basis for the data stored in *Bath* is GEBCO's gridded bathymetric data set: GEBCO 2019 [30]. The data from the dataset was processed after downloading: the data in 'geotiff' format was converted to a georeferenced data grid using the 'geotiffread' function and then it was down sized to 20% using the built-in 'resizem' function. Data is currently only stored for the North, Norwegain and Barents Sea: latitude 47° N to 75° N and −10° E to 30° E.

Within *PipeProf* a profile is generated using the *mapprofile* function and the *POI* defined in *Case*, which must be given in decimal degrees. The profile generated reflects the contours of the seabed and not necessarily a realistic pipeline route, which would be designed to avoid abrupt changes in direction. To reflect this, the raw profile data is smoothed before it is used in the pressure drop calculations.

To ensure that the method described above gives a realistic result for the pipeline profile, published profile data from the Melkøya CO_2 pipeline [31] was used in a qualitative validation exercise, which is presented in Figure 2. The method used in the validation exercise was to define a pipeline based on the information contained in [31] and then to automatically generate a pipeline profile from the bathymetry data stored in the model. The modelled pipeline elevation profile could then be compared to the pipeline elevation profile presented in [31] to check consistency. The results of this comparison as illustrated in Figure 2.

(**a**)   (**b**)
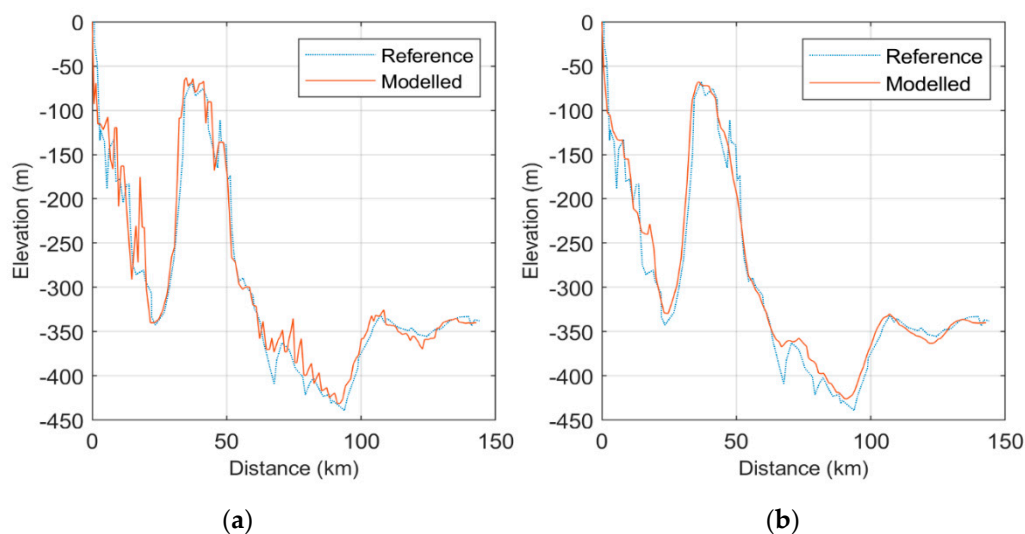
Figure 2. Elevation Profile Comparison Between Reference Data for Melkøya; [31] and (**a**) Modelled Profile with no Smoothing; (**b**) Profile with Smoothing.

To allow the comparison of pipeline operating conditions in different geographic locations the model calculates the average sea temperature for the pipeline, T_{sea}, based on Sea Surface Temperature (SST) data for the 10 year period April 2009 to April 2019. The data was obtained from Japan Meteorological Association (JMA) [32] and is stored in the model as the file *SSTdata*.

In the development of the model, raw data from JMA was converted to NetCFD format for easy use, and trimmed to cover only the area of interest. Monthly averaged data was then used to determine the mean SST value at each grid point. A value of SST equal to mean plus two standard deviations was then calculated to set a realistic maximum pipeline design operating temperature that reflects 97.5% of the monthly averaged data.

In reality, the temperature of the seawater below the surface will normally be several degrees lower than SST. This reduction in temperature below SST is difficult to generalize, and is therefore, not

used in the model. To allow flexibility, the option to manually set a value for T_{sea} is provided via the parameter T_{sea} in *Case*.

2.3. Pipeline Pressure and Temperature Profiles

Both the pipeline pressure and temperature profiles are generated by the *PressProf* function which uses the results from *PipeProf* and data for the *Stream* specified in *Case*. The procedure contained in *PressProf* is a numerical stepwise approach to the calculation of the pipeline pressure profile,

$$P_{out} = P_{in} - \sum \left(P_n^f - P_n^s\right), \tag{1}$$

where P_{out} is the pipeline outlet pressure, P_{in} is the pipeline inlet pressure, P_n^f is the frictional pressure drop for the element n in the pipeline and P_n^s is the static pressure change for elmenet n. The calculation methods associated with static and frictional pressure change are detailed under later headings.

The calculation procedure for P_{out} begins with an estimate for P_{in} and continues stepwise with the pressure in each element 'n' calculated based on the pressure in the previous element. When the pipeline pressure calculation has been completed, the calculated value of P_{out} is compared to the WHP and the minimum allowable pipeline pressure along the full length of the pipeline, P_n^{min}, and a correction is made to the estimated value of P_{in}:

$$C = \max\left(\text{WHP} - P_{out} \ \& \ P_n^{min} - P_n\right), \tag{2}$$

$$\text{and } P_{in} = P_{in} + C, \tag{3}$$

where C is a correction factor used in the calculation algorithm. The pressure drop calculation then continues iteratively until the absolute value of C is less than 1 bar. The calculation of WHP and P_n^{min} is described under the next two headings.

2.3.1. Well Head Pressure

Studies such as that of Maldal [33] and Shi et al. [34] illustrate that CO_2 reservoir pressure will normally change substantially over time, varying with reservoir conditions and operating parameters such as flowrate. This makes the selection of a representative modelling basis for WHP complicated. The approach taken in this study was, therefore, to assess the range of likely reservoir pressure conditions across the lifespan of storage reservoir from limiting cases. For example, Vishal et al. [35] state that "*Depending on the national regulatory, maximum allowed [over] pressure generally corresponds to the 50% of the initial hydrostatic pressure or the 60% of initial lithostatic pressure at the top of the storage formation*". Accordingly, the model present results for three cases where the reservoir pressure is set at 10%, 30% and 50% above initial hydrostatic pressure, which is calculated from the *Res_Depth* parameter in *Case*,

$$P_R = \rho_w \cdot h \cdot g \cdot 10^{-5}, \tag{4}$$

where P_R (bar) is the reservoir pressure, ρ_w is the density of water (kg/m^3) and h is the depth of the reservoir (m) and g is the gravitational constant (m/s^2).

Frictional pressure loss in the pipework associated with the well depends on the length of the well, its diameter and the injection rate, which in-turn depends on the number of injection wells. In this work, for simplicity, the wellhead frictional pressure drop has been based on the Norsok Standard, P-100, which calls for a pressure drop of 0.11–0.27 bar/100 m for wells operating 35–138 barg. WHP is calculated by dividing the well pipework into 100 elements and summating the static head change and frictional pressure loss in each element,

$$\text{WHP} = P_R R + \sum_{i=1}^{100} h_i \left(\rho_i \cdot g \cdot 10^{-5} - P_W^f \ 10^{-2}\right), \tag{5}$$

where R is the overpressure ratio (1.1, 1.3 and 1.5 being the default values in the model), h_i is the height of element i in the well pipework, ρ_n is the density of the CO_2 mixture in element (kg/m^3) and P_W^f is a constant frictional loss = 0.15 bar/100 m for the pipework associated with the well(s).

2.3.2. Minimum Pipeline Operating Pressure

CO_2 pipelines are often designed based on a minimum operating pressure that is set at a margin above the critical pressure of the CO_2 mixture present in the pipeline [3,14,36], as illustrated below by the green dashed line in Figure 3. The purpose this is to avoid a situation where a pipeline operating in the supercritical region cools to conditions close to the critical point—where density can be difficult to predict—or, worse still, where pipelines operating in the gas phase cool leading to condensation. However, sub-sea pipelines located in the North, Norwegian and Barents Sea can be expected to operate with CO_2 in the dense phase, i.e., well below the critical temperature of CO_2 (31 °C). Under these conditions, phase change can be avoided by specifying a minimum approach to the bubble point curve as illustrated by the blue dashed line in Figure 3.
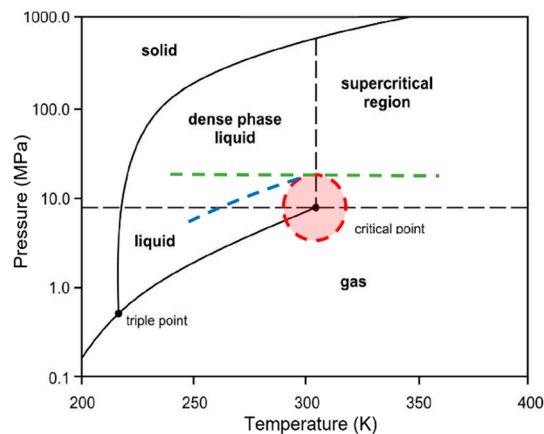
Figure 3. Illustration of Pipeline Operational Limits.

The model calculates the minimum operating pressure for each element in the pipeline as part of the pressure profile calculations in the *PressProf* function using a 10 bar margin to the bubble point pressure,

$$P_n^{\min} = P_n^{BP} + 10 \text{ bar} \tag{6}$$

where $P_n^{\min}$ is the minimum operating press in element n and P_n^{BP} is the bubble point pressure of the mixture in the pipeline at element n. Accurate prediction of the P_n^{BP} of each CO_2 mixture is important to the specification of $P_n^{\min}$ and to ensure this, bubble point data from the TREND properties package [7] is used as the basis for the model. This basis data is stored in the files *Post*, *Pre* and *Oxy* as a set of gridded interpolation data.

2.3.3. Pipeline Diameter Selection

Several studies have presented methods for determining the optimim diameter for CO_2 pipelines [14–16], which is normally based on minimising costs. Others have proposed that "the smallest diameter which ensures that pressure drops are lower than the maximum allowable pressure is the cost-optimal diameter … " [37], but this only transfers the determination of optimum diameter to that of the determination of the maximum allowable pressure, which has been suggested to lie between 15.3 and 20 MPa [5,15,38,39]. The approach adopted in the model is, therefore, to obviate the difficulties associated with identifying optimum diameter by presenting results for a range of suitable diameters. The range used in a particular case is defined using a minimum inside diameter, $D_{ID}^{\min}$, and the next three larger standard pipe sizes.

$D_{\text{ID}}^{\text{min}}$ is calculated using an erosional velocity limit, u_e, the minimum gas density in the pipeline, ρ_{min}, and the parameter *Flow* from the model input parameters,

$$D_{\text{ID}}^{\text{min}} = \sqrt{\frac{4 \cdot m}{\pi \cdot \rho_{\text{min}} \cdot u_e}} \tag{7}$$

where m is the mass flow in the pipeline (kg/s) based on the parameter *Flow* from *Case*. The erosional velocity limit is, in turn, calculated based on the formula given in API 14C and the factor 'c' taken as 100 for continuous flow [3],

$$u_e = 0.82 \, c / \sqrt{\rho_{\text{min}}} \tag{8}$$

where the minimum gas density, ρ_{min}, is calculated using the worst case for all minimum operating pressure conditions along the pipeline and the minimum SST.

The three standard pipe sizes that lie above $D_{\text{ID}}^{\text{min}}$ are based on 2 inch intervals between the standard pipe sizes. Early testing of the model confirmed that this approach covers all of the sizes that would normally be of interest for study purposes.

The density of the CO_2 mixture is used in several of the calculations carried out by the model and, therefore, accurate prediction at different pressure and temperature conditions is important. To ensure this, density data from the TREND [7] properties package is stored for each of the streams in the files *Post*, *Pre* and *Oxy* as a set of gridded interpolation data.

2.3.4. Calculation of Frictional and Static Pressure Changes

Frictional pressure drop, P_n^f, is calculated in *Press_prof* using the Darcy–Weisbach equation:

$$P_n^f = 2 f_F \frac{L_n}{D_{\text{ID}}} \rho_n^{\text{av}} u_n^2 \tag{9}$$

where f_F is the Fanning friction factor calculated using ρ_n^{av}, L_n is the length of element n, D_{ID} is the inside diameter of the pipeline (4 cases), ρ_n^{av} is the average density in element n and u_n is the average velocity in element n, which is also calculated using ρ_n^{av}.

The calculation of ρ_n^{av} is based on the assumption that, although P_n^f is generally small for short L_n, the static pressure change, P_n^s, can be significant when the elevation change is also significant. Accordingly, the average pressure and density are estimated prior to conducting the pressure drop calculation to improve accuracy using a simple linear average,

$$P_n^{\text{av}} = \frac{1}{2} \left[P_{n-1} + (P_{n-1} + \rho_{n-1} \, g \, El_n) \right] \tag{10}$$

where El_n is the elevation change for the nth element in the pipeline and ρ_{n-1} is the density for the preceding pipeline segment $n - 1$, which is calculated as a function of pressure and temperature.

The static pressure loss in each pipeline segment is calculated using the average density:

$$P_n^s = \rho_n^{\text{av}} g \, El_n. \tag{11}$$

The pressure drop calculations are made step-by-step alongside the temperature profile calculations for the full length of the pipeline. Temperature profile calculations are described under a separate heading.

2.3.5. Pipeline Roughness and Friction Factor

Pipeline roughness and friction factor have an important impact on pressure drop. In common with other studies [14,15], the model described here uses the Zirang and Sylverster equation [40] to

estimate the Fanning friction factor, f_F, which has been shown by Winning and Coole [41] to give good accuracy,

$$\frac{1}{\sqrt{f_F}} = -4\log\left\{\frac{e/D_{\mathrm{ID}}}{3.7} - \frac{5.02}{\mathrm{Re}_n}\log[A]\right\} \tag{12}$$

$$A = \frac{e/D_{\mathrm{ID}}}{3.7} - \frac{5.02}{\mathrm{Re}_n}\log\left[\frac{e/D_{\mathrm{ID}}}{3.7} - \frac{13}{\mathrm{Re}_n}\right] \tag{13}$$

where, e is the pipeline roughness (mm), D_{ID} is as before and, Re_n is the Reynold's number for element n:

$$\mathrm{Re}_n = D_{\mathrm{ID}}\, u_n\, \rho_n^{\mathrm{av}} / \mu_n^{\mathrm{av}}, \tag{14}$$

where μ_n^{av} is the average viscosity of the mixture in element n. The calculation of friction factor is carried out in the model using the *fFact* function; viscosity is calculated based on P_n^{av} and ρ_n^{av} using the function *Visc*, which is based on the Lohrenz, Bray and Clark (LBC) formula with the parameter fitting for CO_2 suggested by Nazeri [9].

The roughness, e, used in Equations (12) and (13) depends on the design of the pipeline. Large-scale gas transport pipelines are typically coated with a thin film of epoxy giving low roughness [42]. Wellong et al. [43], for example, found that for large scale natural gas pipelines "79.1% of the absolute roughness values lie in the region from 5 µm to 15 µm" while Langelandsvik [42] found average roughness of 4 µm. However, studies relating to CO_2 pipelines have often used higher values of e: Mazzoccoli [5] and McCoy [15], for example, use 45.7 µm and Chandel et al. [44] use 100 µm to reflect old pipe. The default value of e used in the model, 15 µm, reflecting that of large natural gas pipelines, but it can be adjusted to suit by the user by specifying *Pipe_e* in *Case*.

2.3.6. Pipeline Temperature Profile

The temperature of the CO_2 entering the pipeline can be expected to vary between cases and with geographic location. If the CO_2 stream entering the pipeline originates from a compressor it will normally be cooled before entering the pipeline to avoid damage to pipeline coatings: A typical limit for inlet temperature being 50 °C [38]. To reflect this, the pipeline inlet temperature is set by default to 5 °C above sea temperature T_{sea} at the pipeline entry. If the CO_2 stream entering the pipeline originates from refrigerated intermediate storage, i.e., arrives at the pipeline entry point via ship, it is then likely to be warmed before entering the pipeline and may enter the pipeline below ambient temperature. In this scenario, the model assumes that the inlet temperature is by default to 5 °C below the average sea temperature T_{sea}. If another inlet temperature is required, or a sensitivity study is to be conducted, the user can set this using *T_inlet* in *Case*.

The temperature of the CO_2 in the pipeline will change in response to both heat loss to ambient and pressure drop along the length of the pipeline. These changes are calculated in the model in parallel to the pressure profile calculations. The calculations are carried out by the *PressProf* function using a heat balance to estimate the losses to ambient and a correction to account for the Joule-Thomson (JT) effect,

$$T_n = T_{\mathrm{sea}} + \left(T_{n-1} - T_{\mathrm{SST}}^{\mathrm{av}}\right)\exp\left\{\frac{-U_o A_{\mathrm{OD}} L_n}{m.Cp_n}\right\} + \mathrm{JT}_n \tag{15}$$

$$\text{and } \mathrm{JT}_n = \alpha(P_n - P_{n-1}), \tag{16}$$

where T_n is the temperature in element n, $T_{\mathrm{SST}}^{\mathrm{av}}$ is the average seawater temperature along the pipeline route, U_o is the overall heat transfer coefficient (W/m²-K), Cp is the specific heat capacity of the CO_2 mixture (J/kg), m is the mass flowrate (kg/s), A_{OD} is the outside area of the pipeline (m²/m), L_n is the length of pipeline element 'n' (m), JT is the JT correction factor (°C), and α is the JT coefficient (°C/bar). The basis for the JT coefficient is tabulated data for the JT coefficient that was derived from Wang et al. [6] and is stored in the model as gridded interpolation function in *Post*, *Pre* and *Oxy*.

The outside area of the pipeline, A_{OD}, is calculated from the D_{ID} and the wall thickness, t:

$$A_{OD} = \pi(D_{ID} + 2t). \tag{17}$$

The wall thickness, t, is estimated using the same method as Chandel et al. [44] and Tian et al. [16]:

$$t = \frac{P^{max}D_{ID}}{2 \cdot S \cdot F \cdot E - P_{max}}, \tag{18}$$

where P^{max} is the maximum allowable operating pressure in the pipeline (based on the pipeline pressure profile), D_{ID} is the pipeline inside diameter (i.e., represents the four selected pipeline sizes for each case), S is the minimum yield strength of the pipeline, F is a design factor and E is a longitudinal joint factor. S, F and E are set to 483 MPa, 0.71 and 1.0 based on Tian et al. [16].

The pipeline heat transfer coefficient, U_o, depends on conditions inside the pipeline, outside the pipeline and on the pipeline design itself (e.g., coating, insulation, etc.). In particular, it depends on whether the pipeline is buried or in direct contact with seawater: Drescher, et al. [10] found that the heat transfer coefficient for pipelines with water as the surrounding substance were, on average, 44.7 W/m^2-K, whereas a coefficient in the range 1 to 6 W/m^2-K have been used in the studies referenced here relating to buried onshore pipework [5,36]. In the present model, a single value of U_o can be set by the user for the full length of the pipeline using the parameter *U* in *Case*. By default, the parameter *U* is to a value of 4 W/m^2-K, but this can be altered by the user when specifying *Case*.

2.3.7. Transportation Energy Consumption

The energy consumption resulting from the transportation of CO_2 in a pipeline depends on the inlet pressure of the pipeline and the temperature of the cooling utility available to the compression or liquefaction processes. The type of transportation process used in the model is set using the parameter *Opt* in *Case*.

If the transportation type specified is 'pipe', the energy consumption is calculated based on the results of earlier modelling work [21], which is stored within the model as tabulated data for the variation in energy consumption with compressor discharge pressure and cooling temperature. The pipeline inlet pressure used to calculate the energy consumption is given by the pipeline pressure profile and the cooling temperature is set by assuming a compressor aftercooler temperature is 5 °C above the SST at the pipeline inlet location.

If the transportation type specified is 'ship', the energy consumption for transportation is the sum of the energy required for liquefaction of the CO_2 at the point of origin of the CO_2 stream and the power required to pump the CO_2 up to the pipeline inlet pressure at the point of deliver to the pipeline. The energy consumption associated with the liquefaction process is, again, based on earlier related modelling work [22], which is stored within the model as tabulated data for the variation in energy consumption with ambient temperature. The liquefaction pressure in this case is fixed at 15 bara and, therefore, energy consumption is determined using only the sea temperature in the geographic location of the liquefaction process. The energy consumption for pumping liquid CO_2 to the required pipeline inlet pressure is calculated based on a set of tabulated performance data for a pump with an adiabatic efficiency of 80% and pure CO_2 as the working fluid.

Figure 4 presents a sample of the data used as the basis for the energy consumption for transportation. The complete set of data is also freely available from previously published works [21,22].

(**a**)   (**b**)
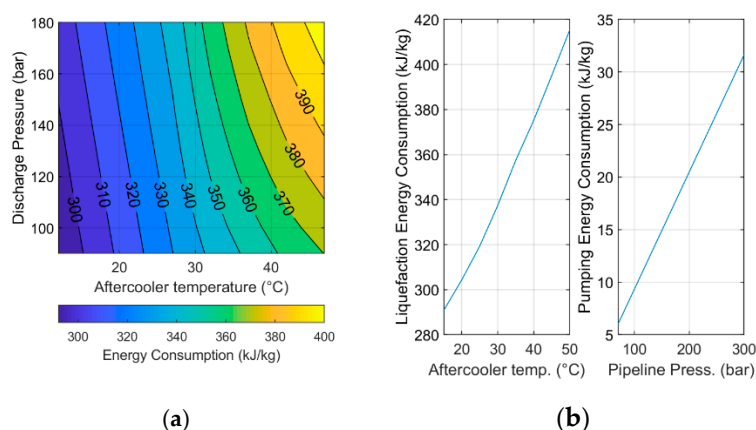
Figure 4. Modeling Basis for the Energy Consumption for Compression, (**a**) Liquefaction and Pumping Power (**b**).

2.4. Model Outputs

Based on the input parameters summarized in Table 2, the model generates a set of outputs, which are summarized in Table 4. These outputs can be subsequently used to automatically generate several plots, as summarized in Table 5, by specifying the *Plot* parameter in *Main*.

Table 4. Summary of Model Outputs.

Name	Profiles
Elevation	Pipeline element length & element elevation change
Pressure	Pressure profile for 10%, 30% & 50% overpressure
Temperature	Pressure profile for 10%, 30% & 50% overpressure

Name	Performance
Inlet Pressure	Inlet pressure for each pipeline size & overpressure case
WHP	Well head pressure for each overpressure case
Av. Frictional DP	Simple mean of frictional pressure drop component for each case
Av. Velocity	Simple mean of gas velocity pressure drop component for each case
Energy	Summary of energy consumption for each pipeline size & overpressure case.

Table 5. Summary Plots Generated by the Model.

Name	Description
Map	Location map for the pipeline/liquefaction location
Conditions	Plot of temperature vs pressure for all pipe sizes and overpressure cases
Profiles	Pressure and temperature profiles for the smallest line size that operates under 200 bar under all conditions
Energy	Sum of pipeline and liquefaction energy consumption for all pipe sizes and overpressure cases

2.5. Model Validation

The aim of the model validation work was to verify the reliability of the pressure and temperature profile calculations carried out by the model. The method chosen was to use the Aspen HYSYS software package, in order to generate a set of reference data against which the pressure and temperature profile predictions made by the model could be compared. The HYSYS software is a process modeling package that is widely used in the gas processing industry that includes a set of built-in modelling capabilities that are suitable for calculating pipeline pressure and temperature profiles, making it well suited to the validation exercise. The approach taken to the assessment of the validation results was to calculate the absolute value of the pressure and temperature error. The limit for an acceptable validation results was

set as an average absolute error of less than 1 °C for the temperature profile and 1 bar for the pressure profile. Further details of the method used in the validation work is presented below.

As the model automatically generates a case-dependent elevation profile that often consists of more than 100 data points it was necessary to construct a simplified profile that could be manually implemented in HYSYS. The simplified profile was created by sampling 19 data points from the Melkøya profile that capture the key features and is stored in a custom case definition called *Validation* which is saved with the model and can be run using *Main*. This validation elevation profile is illustrated in Figure 2 and the data points that form the basis are presented in Table 6.

Table 6. Elevation Profile Used in the Validation.

Length (km)	Elevation (m)	Length (km)	Elevation (m)
0.0	0.0	58.7	−310
0.4	−1.2	65.1	−371
0.5	−99.1	76.1	−384
3.1	−127	91.4	−435
18.0	−228	107	−343
21.3	−230	126	−363
25.5	−338	133	−344
39.7	−65.4	145	−341
47.1	−102	149	−321
53.7	−317	152	−322

In the HYSYS model, the Peng Robinson (PR) properties package was used with default options and the mixture in the pipeline was considered to be pure CO_2. In the model, to allow a direct comparison with the HYSYS results, a set of density and heat capacity data was generated from HYSYS that formed the modelling basis for the validation work. This data is stored in the model as a stream called *Post_Val*.

The inlet pressure calculated by the model was then used to specify the inlet pressure in the HYSYS model so that the results could be directly compared. The results of this validation exercise are stored in full with the model, which is available at UiT Open Research Data [45] and presented below in the Results section.

2.6. Sample Case

As described under earlier headings, the normal basis for the density and heat capacity calculations made by the model is tabulated data from the TREND properties package. Therefore, because the results from the validation study are based on properties data generated using HYSYS, the results are not directly equivalent to the standard model output for the same input parameters. To provide a comparison against the model results for the same case, a sample set of results were generated using the case file called Melkoya, which has the same input parameters as Validation. These results are saved in full with the model available at UiT Open Research Data [45] and can also be generated by running Main with Validation selected as the example case. A summary of these results is presented in the Results.

3. Results

The results provided here are limited to the presentation of a summary of the findings of the validation exercise and the presentation of a single set of results for a Sample Case: the Melkøya CO_2 pipeline using a rough interpretation of the pipeline route from Såtendal et al. [31]. Full results for both of these cases are stored with the model at UiT Open Research Data [45].

3.1. Validation

Figure 5 provides a comparison of the temperature profile generated by the model and HYSYS for the same validation case. Figure 5b shows that the average absolute temperature difference between

the two models is less than 1 °C, which indicates that the calculations made by the model are reliable. Figure 6 provides a comparison of the pressure profile generated by the model and HYSYS for the same validation case. Again, the results from the model correspond well with the results from the HYSYS model, with a maximum pressure difference of under 1 bar across the full length of the pipeline.

(a)   (b)
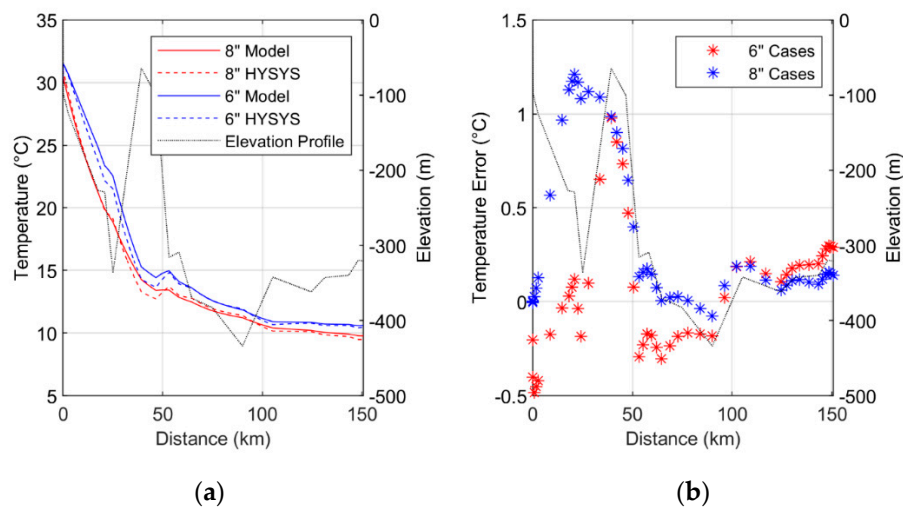
Figure 5. Comparison of Model and HYSYS Results for the Validation Case, (**a**) shows a Comparison of the Temperature Profile Results for the 10% Overpressure Case; and (**b**) shows the Absolute Temperature Difference Between the Results.

(a)   (b)
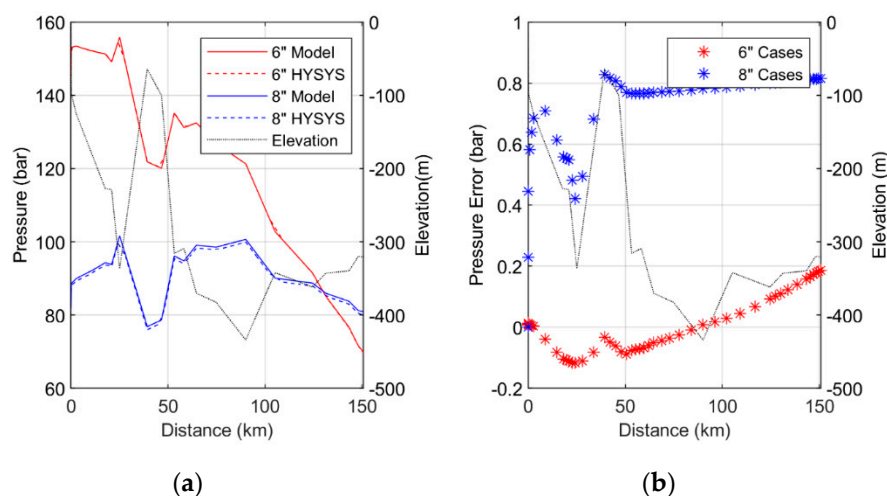
Figure 6. Comparison of Model and HYSYS Results for the Validation Case: (**a**) Shows a Comparison of the Pressure Profile Results for the 10% Overpressure Case; and (**b**) Shows the Absolute Pressure Difference Between the Two Sets of Results.

3.2. Sample Case

Figures 7–10 present the standard set of model plots as described by Table 4. Figure 9 shows that the smallest pipeline size to ensure operating conditions under 200 bar in all operating cases is 8 inches. Figure 9 also shows that a margin is maintained against the bubble point pressure for all cases across the pipeline length. Figure 10 shows the temperature and pressure profiles for the 10% reservoir overpressure case and illustrates that the minimum pressure condition at the wellhead end only dictates the pipeline inlet pressure for the 6 inch pipeline case due to high pressure drop along the pipeline. In the other cases the minimum pipeline pressure condition (approach to the bubble point

pressure) sets the pipeline inlet pressure, which means that some pressure letdown would be required at the wellhead to reach WHP.
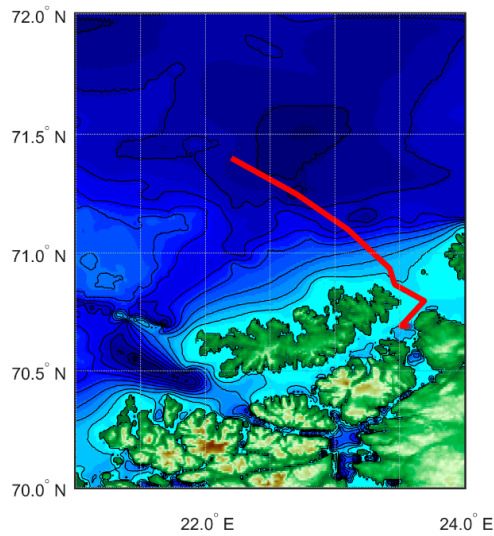
Figure 7. Approximate Melkøya CO_2 Pipeline Route.
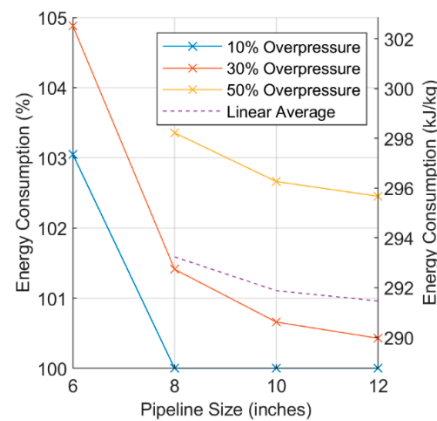
Figure 8. Summary of Energy Consumption for the Melkøya CO_2 Pipeline Example.
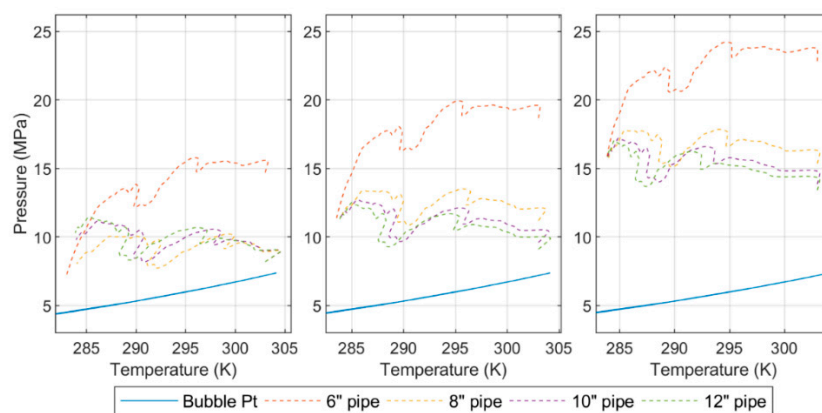
Figure 9. Summary of Pipeline Temperature and Pressure Conditions for the Melkøya CO_2 Pipeline Example. On the left is the 10% reservoir overpressure case, middle 30% and right 50% overpressure.
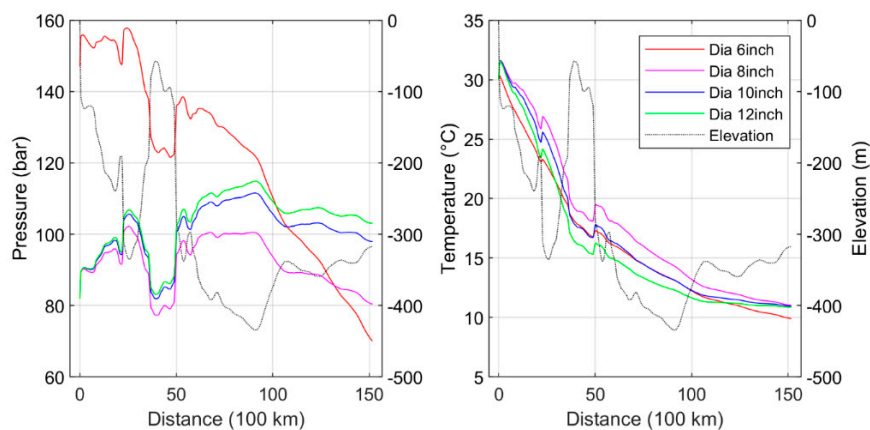
Figure 10. Summary of Pipeline Temperature and Pressure Profiles for the Melkøya CO_2 Pipeline Example for the 10% reservoir overpressure case.

The tabulated data that forms the basis for Figures 5, 6, 9 and 10 is stored with the model and available at UiT Open Research Data [45]. The raw data allows a more detailed comparison of the results obtained using the modelling basis for the validation work (illustrated in Figures 5 and 6) and the results obtained using the standard modelling basis (presented in Figures 9 and 10). For example, the data for the 6 inch line size and the 10% overpressure case shows that the inlet pressure is 144.4 bar in the validation results and 147.0 bar for the default model. A comparison of the 8 inch line outlet pressure for the 10% overpressure case shows 80.9 bar for the validation case and 80.4 bar for the default model basis. Outlet temperatures are also very similar in all cases.

4. Discussions

The scope of this article is the development and validation of a pipeline model; application of the model to compare the performance of different CO_2 pipeline alternatives will form part of future study work. In particular, the model described here is intended for use in the development of larger system models that will include the performance of the capture element of carbon free value chains.

The model presented here is presently only fully developed for the post and pre combustion CO_2 compositions. Data for the oxyfuel stream composition and transportation energy consumption can be calculated by the model, but this is not on a consistent basis with the pre- and post-combustion cases, and therefore, cannot be directly compared with these cases.

The results of the validation work show that the model can reproduce pipeline pressure profiles with good accuracy and that a representative elevation profile can be generated automatically from bathymetry data that captures the key features of a complicated pipeline route such as the one associated with the Melkøya CO_2 pipeline. A comparison of the validation results to the standard modelling basis also shows good agreement.

5. Conclusions

This article has presented the development of a model for CO_2 transportation processes. The model has been validated and tested against an example case, and can be seen to give consistent results.

The results of the validation work show that the pressure and temperature profile have an average absolute error of less than 1 bar, and 1 °C, respectively compared to the selected reference model supporting the aim of the work, which is to provide a consistent and transparent basis for the comparison of different CO_2 transportation scenarios.

The results from the sample case show how the results of the model can be used to provide useful design and performance information for CO_2 pipelines, confirming, for example, that the installed size of 8 inches [31] is the optimum size for the Melkøya pipeline.

The development of comparisons between different transport case will form the scope of future work. The code for the model presented here along with all the data needed for its use and the results presented in this article is available at UiT Open Research Data [45].

Conflicts of Interest: The authors declare no conflict of interest.

Nomenclature

A	Area based on OD
c	Erosional velocity factor
C	Model correction factor
Cp	Heat capacity
D	Diameter
e	Absolute roughness
E	Pipeline joint factor
F	Pipeline design factor
f_F	Fanning friction factor
g	Gravitational constant
h	Reservoir depth
h	Height
JT	Joule-Thompson coefficient
L	Length
P	Pressure
P	Pressure drop
R	Reservoir overpressure factor
Re	Reynolds number
S	Min. pipeline yield strength
t	Pipe wall thickness
T	Temperature
u	Velocity
U_o	Overall heat transfer coefficient
WHP	Well head pressure
μ	Viscosity
ρ	Density
Subscripts & Superscripts	
av	Average
BP	Bubble point
e	erosion
f	Friction
i	Element 'i' in the well
ID	Based on inside diameter
in	Inlet
max	Max
min	minimum
min	Min
n	Element 'n' in the pipeline
o	Overall
OD	Based on outside diameter
out	Outlet
R	Reservoir
s	Static

sea	Average sea condition
SST	Sea surface temperature
w	Water

References

1. Global CCS Institute. *Global Status of CCS 2019*; Global CCS Institute: Melbourne, Australia, 2019.
2. IEA. *World Energy Outlook 2019*; IEA: Paris, France, 2019. [CrossRef]
3. Peletiri, S.P.; Rahmanian, N.; Mujtaba, I.M. CO_2 Pipeline design: A review. *Energies* **2018**, *11*, 2184. [CrossRef]
4. Northern Lights—A European CO2 Transport and Storage Network. Available online: https://northernlightsccs.eu/ (accessed on 5 March 2020).
5. Mazzoccoli, M.; Bosio, B.; Arato, E.; Brandani, S. Comparison of equations-of-state with P-p-T experimental data of binary mixtures rich in CO_2 under the conditions of pipeline transport. *J. Supercrit. Fluids* **2014**, *95*, 474–490. [CrossRef]
6. Wang, J.; Wang, Z.; Sun, B. Improved equation of CO_2 Joule–Thomson coefficient. *J. CO2 Util.* **2017**, *19*, 296–307. [CrossRef]
7. Span, R.E.T.; Herrig, S.; Hielscher, S.; Jäger, A.; Thol, M. TREND. In *Thermodynamic Reference and Engineering Data 3.0*; Lehrstuhl für Thermodynamik, Ruhr-Universität Bochum: Bochum, Germany, 2016.
8. Wilhelmsena, Ø.; Skaugena, G.; Jørstadb, O.; Hailong, L. Evaluation of SPUNG# and other Equations of State for use in Carbon Capture and Storage modelling. *Energy Procedia* **2012**, *23*, 236–245.
9. Nazeri, M.; Chapoy, A.; Burgass, R.; Tohidi, B. Viscosity of CO_2-rich mixtures from 243 K to 423 K at pressures up to 155 MPa: New experimental viscosity data and modelling. *J. Chem. Thermodyn.* **2018**, *118*, 100–114. [CrossRef]
10. Drescher, M.; Wilhelmsen, Ø.; Aursand, P.; Aursand, E.; de Koeijer, G.; Held, R. Heat Transfer Characteristics of a Pipeline for CO_2 Transport with Water as Surrounding Substance. *Energy Procedia* **2013**, *37*, 3047–3056. [CrossRef]
11. Lee, W.J.; Yun, R. In-tube convective heat transfer characteristics of CO_2 mixtures in a pipeline. *Int. J. Heat Mass Transf.* **2018**, *125*, 350–356. [CrossRef]
12. Wetenhall, B.; Race, J.M.; Aghajani, H.; Barnett, J. The main factors affecting heat transfer along dense phase CO_2 pipelines. *Int. J. Greenh. Gas Control* **2017**, *63*, 86–94. [CrossRef]
13. Zhang, W.B.; Shao, D.; Yan, Y.; Liu, S.; Wang, T. Experimental investigations into the transient behaviours of CO_2 in a horizontal pipeline during flexible CCS operations. *Int. J. Greenh. Gas Control* **2018**, *79*, 193–199. [CrossRef]
14. Mohammadi, M.; Hourfar, F.; Elkamel, A.; Leonenko, Y. Economic Optimization Design of CO_2 Pipeline Transportation with Booster Stations. *Ind. Eng. Chem. Res.* **2019**, *58*, 16730–16742. [CrossRef]
15. McCoy, S.; Rubin, E. An engineering-economic model of pipeline transport of CO_2 with application to carbon capture and storage. *Int. J. Greenh. Gas Control* **2008**, *2*, 219–229. [CrossRef]
16. Tian, Q.; Zhao, D.; Li, Z.; Zhu, Q. Robust and stepwise optimization design for CO_2 pipeline transportation. *Int. J. Greenh. Gas Control* **2017**, *58*, 10–18. [CrossRef]
17. Deng, H.; Roussanaly, S.; Skaugen, G. Techno-economic analyses of CO_2 liquefaction: Impact of product pressure and impurities. *Int. J. Refrig.* **2019**, *103*, 301–315. [CrossRef]
18. Aspelund, A.; Mølnvik, M.J.; De Koeijer, G. Ship Transport of CO_2: Technical Solutions and Analysis of Costs, Energy Utilization, Exergy Efficiency and CO_2 Emissions. *Chem. Eng. Res. Des.* **2006**, *84*, 847–855. [CrossRef]
19. Knoope, M.M.J.; Ramírez, A.; Faaij, A.P.C. Investing in CO_2 transport infrastructure under uncertainty: A comparison between ships and pipelines. *Int. J. Greenh. Gas Control* **2015**, *41*, 174–5836. [CrossRef]
20. Jordal, K.; Aspelund, A. Gas conditioning—The interface between CO_2 capture and transport. *International Int. J. Greenh. Gas Control* **2007**, *1*, 343–354.
21. Jackson, S.; Brodal, E. Optimization of the Energy Consumption of a Carbon Capture and Sequestration Related Carbon Dioxide Compression Processes. *Energies* **2019**, *12*, 1603. [CrossRef]
22. Jackson, S.; Brodal, E. Optimization of the CO_2 Liquefaction Process-Performance Study with Varying Ambient Temperature. *Appl. Sci.* **2019**, *9*, 4467. [CrossRef]
23. Alabdulkarem, A.; Hwang, Y.H.; Radermacher, R. Development of CO_2 liquefaction cycles for CO_2 sequestration. *Appl. Therm. Eng.* **2012**, *33*, 144–156. [CrossRef]

24. Seo, Y.; Huh, C.; Lee, S.; Chang, D. Comparison of CO_2 liquefaction pressures for ship-based carbon capture and storage (CCS) chain. *Int. J. Greenh. Gas Control* **2016**, *52*, 1–12. [CrossRef]

25. Øi, L.E.; Eldrup, N.H.; Adhikari, U.; Bentsen, M.H.; Badalge, J.C.L.; Yang, S. Simulation and Cost Comparison of CO_2 Liquefaction. *Energy Proceida* **2016**, *86*, 500–510. [CrossRef]

26. Jakobsen, J.; Roussanaly, S.; Anantharaman, R. A techno-economic case study of CO_2 capture, transport and storage chain from a cement plant in Norway. *J. Clean. Prod.* **2017**, *144*, 523–539. [CrossRef]

27. Jakobsen, J.P.; Roussanaly, S.; Brunsvold, A.; Anantharaman, R. A Tool for Integrated Multi-criteria Assessment of the CCS Value Chain. *Energy Procedia* **2014**, *63*, 7290–7297. [CrossRef]

28. Mallon, W.; Buit, L.; van Wingerden, J.; Lemmens, H.; Eldrup, N.H. Costs of CO_2 Transportation Infrastructures. *Energy Procedia* **2013**, *37*, 2969–2980. [CrossRef]

29. The MathWorks. *MATLAB*; The MathWorks: Natick, MA, USA, 2018.

30. GEBCO Compilation Group. GEBCO 2019 Grid. 2019. Available online: https://www.gebco.net/data_and_products/gridded_bathymetry_data/gebco_2019/gebco_2019_info.html (accessed on 27 January 2020).

31. Såtendal, S.H.; Laug, R.; Oaland, O. Subsea Pipeline Intervention In the Barents Sea. In Proceedings of the Seventeenth International Offshore and Polar Engineering Conference, Lisbon, Portugal, 1 January 2007; p. 7.

32. Japan Meteorological Agency. Available online: http://ds.data.jma.go.jp/tcc/tcc/products/elnino/cobesst_doc.html (accessed on 1 November 2019).

33. Maldal, T.; Tappel, I.M. CO_2 underground storage for Snøhvit gas field development. *Energy* **2004**, *29*, 1403–1411. [CrossRef]

34. Shi, J.-Q.; Imrie, C.; Sinayuc, C.; Durucan, S.; Korre, A.; Eiken, O. Snøhvit CO_2 Storage Project: Assessment of CO_2 Injection Performance Through History Matching of the Injection Well Pressure Over a 32-months Period. *Energy Procedia* **2013**, *37*, 3267–3274. [CrossRef]

35. Vishal, V.; Singh, T.N. *Geologic Carbon Sequestration: Understanding Reservoir Behavior*; Springer Nature: Cham, Switzerland, 2016. [CrossRef]

36. Zhang, Z.X.; Wang, G.X.; Massarotto, P.; Rudolph, V. Optimization of pipeline transport for CO_2 sequestration. *Energy Convers. Manag.* **2006**, *47*, 702–715. [CrossRef]

37. Roussanaly, S.; Brunsvold, A.L.; Hognes, E.S. Benchmarking of CO_2 transport technologies: Part II – Offshore pipeline and shipping to an offshore site. *Int. J. Greenh. Gas Control* **2014**, *28*, 283–299. [CrossRef]

38. Nimtz, M.; Klatt, M.; Wiese, B.; Kühn, M.; Joachim Krautz, H. Modelling of the CO_2 process- and transport chain in CCS systems—Examination of transport and storage processes. *Geochemistry* **2010**, *70*, 185–192. [CrossRef]

39. Forbes, S.M.; Verma, P.; Curry, T.E.; Friedmann, S.J.; Wade, S.M. *CCS Guidelines: Guidelines for Carbon Dioxide Capture, Transport, and Storage*; World Resources Institute: Washington, DC, USA, 2008.

40. Zigrang, D.; Sylvester, N. Explicit approximations to the solution of Colebrook's friction factor equation. *AIChE J.* **1982**, *28*, 514–515. [CrossRef]

41. Winning, H.; Coole, T. Explicit Friction Factor Accuracy and Computational Efficiency for Turbulent Flow in Pipes. *Int. J. Publ. Assoc. ERCOFTAC* **2013**, *90*, 1–27. [CrossRef]

42. Langelandsvik, L.I. *Modeling of Natural Gas Transport and Friction Factor for Large-Scale Pipelines: Laboratory Experiments and Analysis of Operational Data*; Norwegian University of Science and Technology, Faculty of Engineering Science and Technology, Department of Energy and Process Engineering: Trondheim, Norway, 2008.

43. Jia, W.; Li, C.; Wu, X. Internal Surface Absolute Roughness for Large-Diameter Natural Gas Transmission Pipelines. *Oil Gas. Eur. Mag.* **2014**, *40*, 211–213.

44. Chandel, M.K.; Pratson, L.F.; Williams, E. Potential economies of scale in CO_2 transport through use of a trunk pipeline. *Energy Convers. Manag.* **2010**, *51*, 2825–2834. [CrossRef]

45. Jackson, S. *Carbon Dioxide Transportation Energy Model*; Version 1, UiT; The Arctic University of Norway, Ed.; DataverseNO: Tromsø, Norway, 2020. [CrossRef]